Repair of acrylic/glass composites by liquid resin injection and press moulding

Repair of acrylic/glass composites by liquid resin injection and press moulding

Alp BOLLUK, Machar Devine, James A. Quinn, Dipa Ray*

School of Engineering, Institute for Materials and Processes, The University of Edinburgh, Sanderson Building, Robert Stevenson Road, Edinburgh, EH9 3FB, Scotland, United Kingdom.

*Corresponding author. Email address: dipa.roy@ed.ac.uk

Keywords: A. Thermoplastic resin; B. Repair; C. Double cantilever beam testing; D. Fracture toughness; Micrographs.

Abstract: This paper presents repair methods for *in-situ* polymerised acrylic (Elium®)/glass composites focusing on mode-I fracture toughness recovery. Acrylic/glass composites were first subjected to double cantilever beam (DCB) tests to measure their Mode-I fracture toughness. The delaminated samples after DCB tests were repaired and rejoined. Two repair methods were performed: liquid resin injection and press moulding at two different temperatures (130°C and 160°C). The repaired samples were subjected to a second set of DCB tests. The fracture behaviours of the four specimen groups (virgin, resin-injected, pressed at 130°C, and pressed at 160°C) were evaluated in terms of strain energy release rates (G_{IC}) during crack initiation and propagation. The results showed that specimens repaired by resin injection exhibited highest G_{IC} values, about 30% higher than the virgin state, due to the formation of a semi-interpenetrating polymer network (semi-IPN) at the joining interface. Scanning electron microscopy images provided insight into distinctive fracture behaviours for each test group.

1. Introduction:

The wind energy sector has used non-recyclable thermoset composites in their blade structures for decades and that has created a huge amount of waste that is currently going to landfill. It is estimated that global annual waste from wind turbines will reach 2 million tonnes by 2050 and this has raised serious concerns in terms of its detrimental impact on the environment. The focus is now growing on recyclable blades, either from recyclable epoxy based thermoset composites or from thermoplastic composites [1]. In a recent project in 2021, ZEBRA (Zero wastE Blade ReseArch), the world's first and largest thermoplastic composite blade prototype has been manufactured using liquid acrylic resin Arkema (Elium), offering full recyclability at the end-of-life. In addition to recyclability, large thermoplastic composite structures can also undergo efficient repair during their service life that can extend their lifetime.

During their service life, composites structures undergo different types of loading and unloading that leads to various levels of delaminations weakening the structure. Upon minor delamination, fibres stay intact, and the laminates' structural integrity is not at risk. However, matrix cracks can trigger further crack propagation leading to failure [2]. Resin injection is a popular method of repair for thermoset composites where low viscosity liquid resins are injected in the damaged area to fill the crack path and seal the damage area, preventing further crack propagation [3]. Hautier et al. repaired T700GC/M21 thermoset composites by infiltrating with RTM6 thermoset resin [4]. The experiment reported an average 50% mode-I fracture toughness recovery, with some of the specimens' crack resistance properties reducing by rates as high as 80%. In a 2019 study, CF/epoxy parts were *co-cured* with different concentrations of polyetherimide (PEI) thermoplastic toughener resin and semi-interpenetrating polymer network (semi-IPN) formations were obtained [5]. A significant increase in fracture toughness (G_{IC}) was recorded with increasing toughener content. However, this study was not a repair investigation. It simply demonstrated positive toughening potential of semi- IPN formation. Semi-IPNs in thermoset systems can only be created if the resins are cured together. If the liquid thermoplastic resin were injected into the cracks of an already cured and cross-linked thermoset composite part, the resulting joint would simply be an adhesive filling with no penetration or molecular bonding with the damaged structure. This is where thermoplastics differ from thermosets, which is essentially the principal driving mechanism of this repair method. Repair by liquid resin injection promises to combine thermoplastic resins' toughening benefits with strong semi-IPN formation in crack areas.

In the case of thermoplastic composites, fusion bonding can also be used as a method of repair where delaminated surfaces are heated under pressure for a defined period of time, and then cooled down to their solidification temperature [6]. Thermoplastics can favour this repair due to their melting and flowability. Upon heating, thermoplastics' long molecular chains gain mobility which allows them to diffuse across the delaminated interfaces under pressure, reproducing a continuous part [7]. Then, with solidification, interlaminar strength and the

integrity of delaminated samples can be restored. Khan et. al. compared fracture toughness of virgin carbon fibre reinforced Elium 188O specimens with counterparts joined (not repaired) under heated press [8]. Authors reported a maximum 65% $G_{IC\text{-}Prop}$ restoration, from 1160 J/m^2 (virgin) to 750 J/m^2 (joined at 210^{o}C, 3 bar and 90 min.). However, even though this technique can be interesting to study in small lab scale, its application is highly restricted by the component size and shape in the real world.

Both liquid resin injection repair and fusion bonding-based repair can be interesting for acrylic based thermoplastic composites. As liquid monomeric acrylic resin is used for manufacturing and it undergoes in-situ polymerisation, this opens up new opportunities especially with liquid resin injection repair. This repair technique works when the liquid resin acts as a reactive solvent for the composite matrix and leads to dissolution of the matrix polymer at the joining interface. This technique is applicable to those composites where the liquid resin used for repair and the matrix polymer are chemically compatible and liquid resin can dissolve or even partially dissolve the substrate matrix. Infusible liquid thermoplastic resins are potential candidates for large recyclable composite structures in future, and hence, this repair technique can become very useful. There is still a gap in knowledge in this area and our work fits in here.

.

This work investigates the repairability of acrylic/glass composites by liquid resin injection repair and conventional heated press repair at two different temperatures. The virgin composite samples were first delaminated via double cantilever beam (DCB) testing, repaired and then tested again via DCB to measure the recovery in the mode-I fracture toughness. The delaminated surfaces were examined under scanning electron microscope (SEM) to observe the crack propagation behaviour in each set of repaired samples.

2. Experimental

2.1 Materials

The material system fabricated as the subject of this study was a glass fibre reinforced acrylic laminate consisting of 4 plies of non-crimp E-glass fabric. The acrylic resin used was *Elium® 188O* from Arkema, France. The resin had a liquid density of 1.01 g/cm^3 and a Brookfield viscosity of 100 MPa.s at 25ºC. The acrylic resin was mixed with BP-50-FT organic peroxide initiator (supplied by United Initiators) in a 100:3 ratio by weight. The E-glass fabric was provided by Saertex/Johns Manville. The 0º and 90º fibres and synthetic stitching weighed 1152, 35 and 13 g/m^2 respectively, summing up to a total areal weight of 1200 g/m^2.

2.2 Laminate Fabrication

Laminates were fabricated via the vacuum-assisted resin infusion (VARI) process. Each laminate consisted of 4 plies of E-glass fabric, each of 0.95 mm thickness, which were cut to be 400 mm in length and 190 mm width. During the layup of the plies, as per ASTM D5528 standard, a polymer non-adhesive pre-crack film of 13 μm (Swiss Composite Shop SCS HT) was cut to 136x150 mm dimensions and was inserted at the midplane of the laminate (between the second and third layers). This film is needed to initiate a crack away from the load introduction point to avoid large deflections as per the guidance, so that accurate values of strain energy release rate can be computed. The film was placed at the laminate mid plane to satisfy the recommended standard pre-crack distance of 63 mm. The plies were oriented such that the two surfaces at the mid plane enabled a delamination growth in the 0º direction.

2.3 Mode-I Fracture Toughness Testing of Virgin Specimens

Double cantilever beam (DCB) testing was conducted on an *Instron 3369* test frame in compliance with *ASTM D5528* standard. Samples were carefully cut from the test laminate to maintain the length of the original initiation site and dimensions (175 mm × 25 mm). Steel loading blocks (25 mm × 25 mm × 15 mm) were bonded to the pre-cracked sample ends for load introduction and high-contrast speckles were applied to sample edges to facilitate automatic tracking. The test machine was equipped with grips where specimens were fitted via the bonded loading blocks. A 10 kN load cell was kept fitted throughout all experiments

and a constant extension rate of 5 mm/min was employed to pull the specimens apart. Load, opening (crosshead) displacement and delamination length were recorded. Video extensometry (Imetrum DIC) was used for automatic detection of crack onset and tracking of delamination length at each instance while the specimens were gradually split open. For each test, loading was performed until a minimum 50 mm delamination was obtained (starting from pre-crack tip), accounting for a total minimum crack length $a = a_0 + 50mm$ from loading point. Modified Beam Theory (MBT) is the most frequently reported method in literature for the calculation of critical strain energy rate, propagation G_{IC}. Also, this method is identified to produce most conservative results in numerous studies and is recommended by ASTM 5528. Hence, MBT was used in the calculation of mode-I fracture toughness of 4 specimen groups. The detailed method is described in the supplementary document. The schematics and details of the DCB samples are added in the supplementary document (Fig. S1, Fig. S2 and Table S1).

2.3 SEM

The fracture behaviour of DCB-tested specimens was examined on a JEOL (JSM-IT100) scanning electron microscope. The interlaminar fracture surfaces were prepared with a 40nm sputter coating of gold to increase conductivity and were imaged at 15 kV.

2.4 Liquid Resin Injection Repair

The liquid resin injection repair was designed based on the findings of a recently filed patent by the University of Edinburgh on joining thermoplastic articles [9]. Since acrylic resin is initially available in monomeric form, this finding further increased the injection repair process' potential in recovering GF/acrylic composites' mode-I fracture toughness. The injected monomeric resin can therefore behave as a reactive solvent upon contact with the thermoplastic acrylic matrix. The applied liquid resin dissolves the contact region and penetrates the composite's matrix, up to an extent. With the consequent polymerization of the added material, the new polymer section creates a unified/homogeneous semi-interpenetrating polymer network with the composite. Semi-interpenetrating polymer network

(semi-IPN) means a polymer blend system where one monomer polymerises and forms a new network in the presence of an existing polymer network. In our case the infused liquid resin at the joining interface forms the new network and the existing polymer network is the substrate acrylic matrix. The semi-IPN formed at the interface is imparting an additional strength to the joining interface. In this way, a tougher interfacial joining is achieved, compared to traditional methods such as welding or adhesive bonding. The repair of damaged thermoplastic composites via liquid thermoplastic resin injection promises to combine these resins' toughening benefits with semi-interpenetrating network formation in crack areas.

The resin-catalyst mixture was drawn into a syringe of 1 mm needle diameter (Figure 1) and injected into the separated mid planes of specimens, one specimen at a time, from the pre-crack film tip (Figure 2). Figure 2 shows schematically the injection repair process and formation of a semi-IPN at the joining interface. Step 1 in Figure 2 shows the injection of the liquid monomeric resin at the debonded interface. The acrylic monomeric resin dissolves the acrylic matrix at the interface and penetrates within the adjacent layer, as shown in step 2. It then polymerises forming a semi-IPN. The interpenetrating network structure at the joining interface makes it stronger than the bulk composite.

A careful attention was paid to keep the film and the pre-crack area resin-free, for accurate repeatability of DCB tests. Acrylic resin's low viscosity properties provided ease in transferring the resin from the source into the needle and from the needle into cracks.

The resin injection was performed from both edges of the specimens until resin was observed to flow outside the opposite edge, ensuring the resin was fully spread into the crack. Overflowed resin was then wiped off from specimens' edges. The openings at the very end of cracks were too small for the needle to reach. Hence, specimens were held vertically, along injection direction, for the resin to reach these areas under gravity.

Fig. 1. *Preparation of injection repair process*

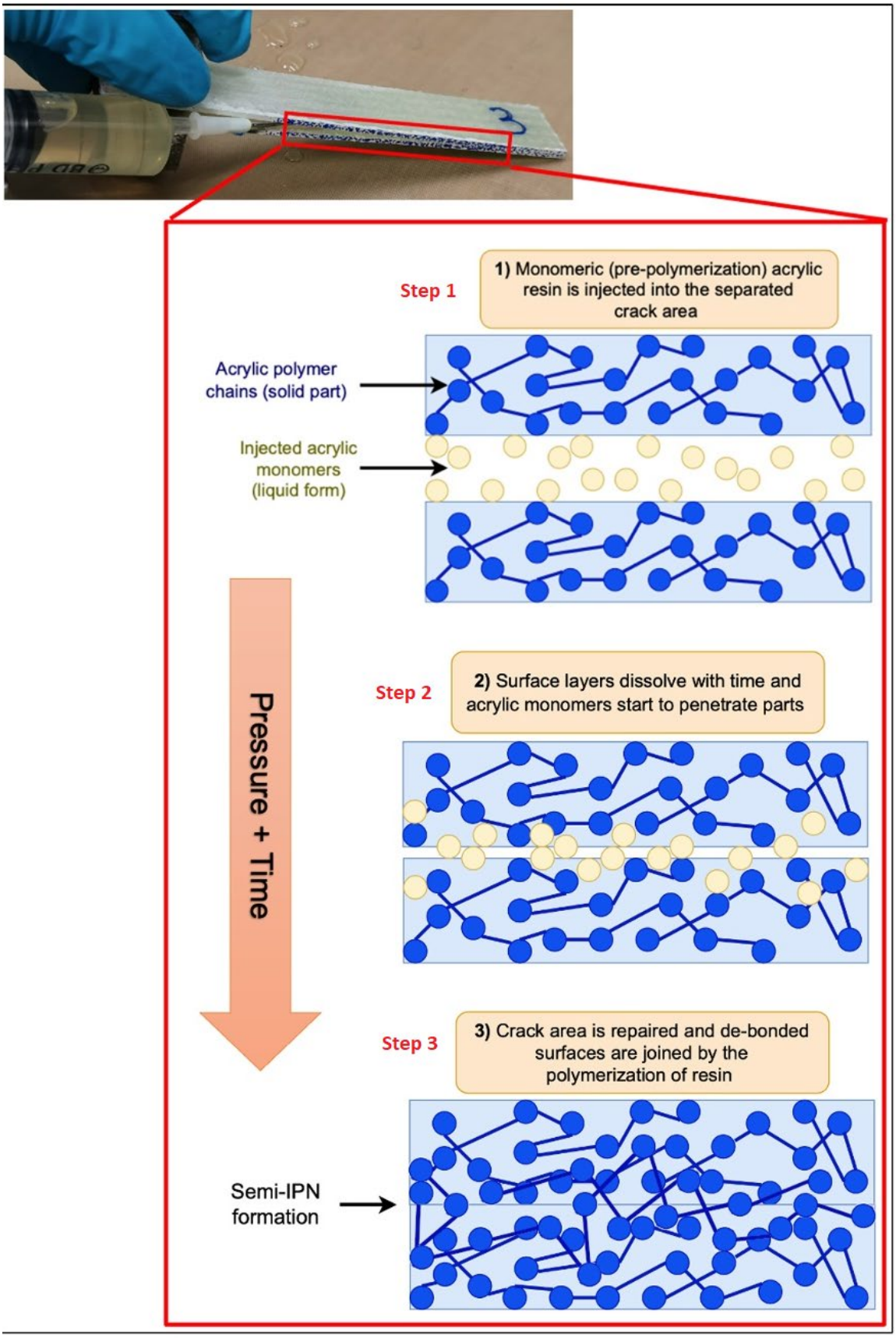

Fig. 2: *A schematic showing acrylic resin injection into separated midplane of the sample and consequent semi-IPN formation*

Injected specimens were aligned on one edge of a 350x350 mm steel plate on which a strip of sealant tape was applied for firm attachment. A non-stick Teflon layer was placed between the specimens and the plate to preserve the steel surface from resin drippings (Figure 3a). The assembly was then transferred onto an 800x800 mm vacuum bag, which was folded over the setup to fully enclose specimens and the plate. (Figure 3b).

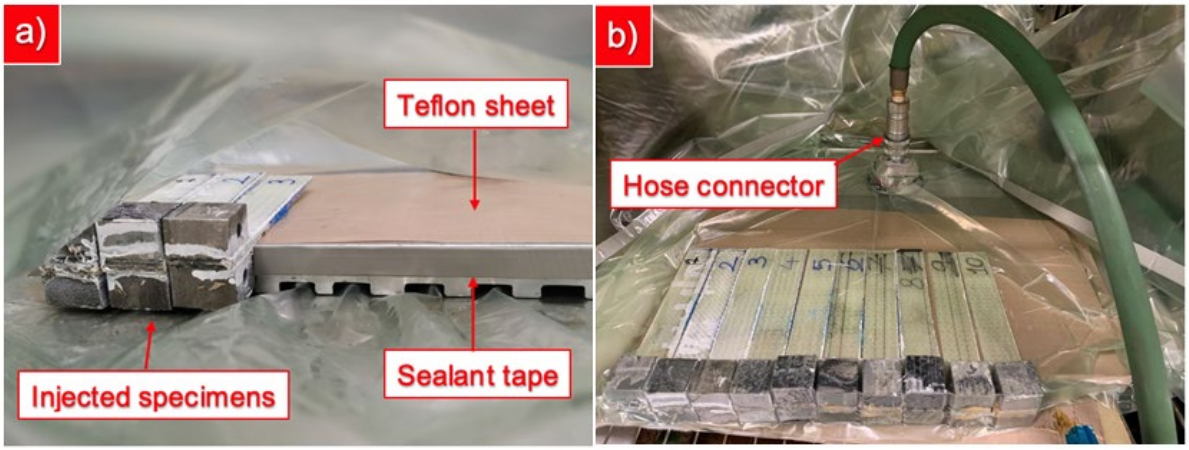

Fig. 3. *a) Lay-up of specimens on repair set-up; b) Assembly with vacuum bag and hose connection*

The injected acrylic resin was left to polymerise *in-situ* overnight in the crack areas, forming rigid semi-IPN connections across the debonded substrate surfaces. Finally, repaired specimens were disassembled from the setup and pre-crack regions were ensured to be still open. The resin injection repair schematic is shown in Figure 4.

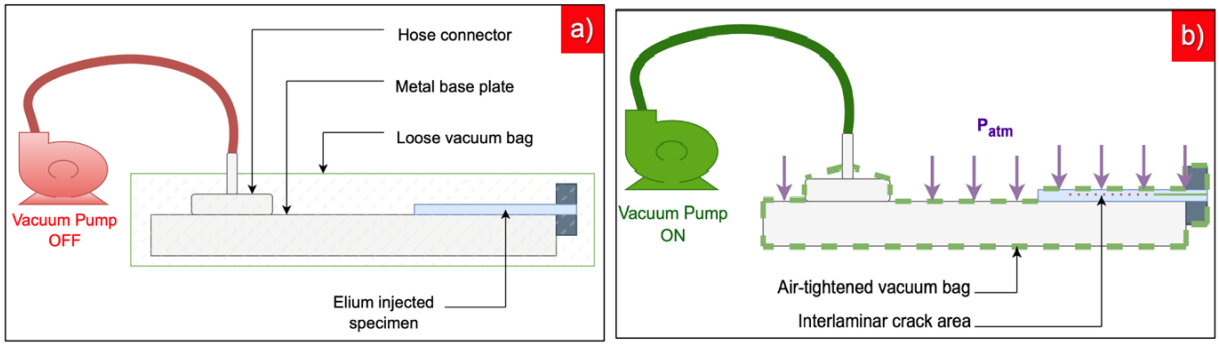

Fig. 4. *Schematic diagram of repair set-up with vacuum pump a) turned off; b) turned on*

2.5 Heated Press Repair

Ten DCB tested specimens were subjected to heated press repair to achieve fusion bonding of separated crack surfaces and restoration of fracture toughness properties. In the aforementioned 2022 study [8], CF/Elium188O composite parts were manufactured via VARI method, consolidated under hot press, and subjected to DCB tests. This was used as the primary reference in determining temperature, pressure, and time parameters.

The press repairs were performed on a PEI Lab 450 Hydraulic Press with active cooling. Two sets of parameters were used for the repair activity. The DCB debonded specimens were placed between two separate pairs of steel plates, around the edges, in a manner that loading blocks were left hanging outside the plates, to be excluded from the pressed area (schematically shown in Figure 5).

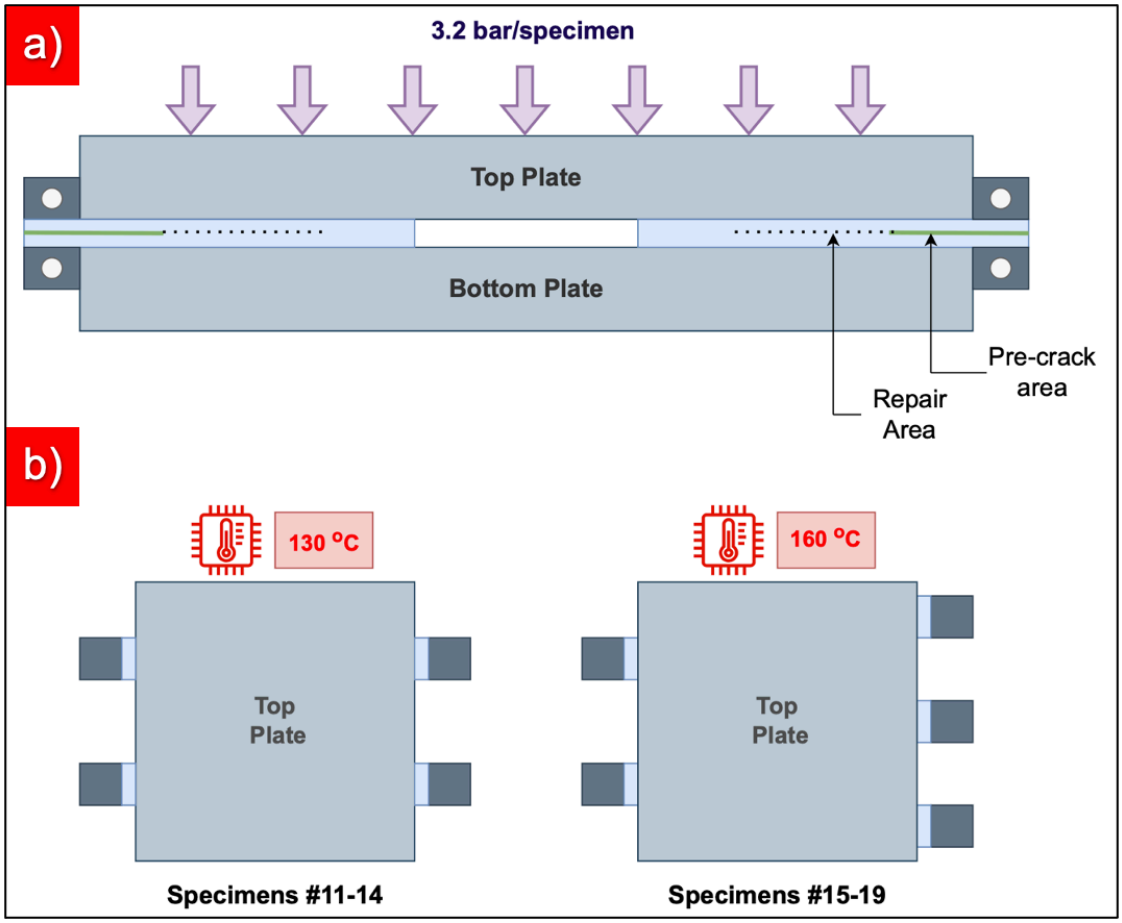

Fig. 5. *Schematic diagram of heated press setup a) side view; b) plan view; (not for scale)*

The process was performed in 3 distinctive stages to induce fusion bonding of the debonded mid plane, while maintaining total load throughout. Heating was from 30ºC to 130ºC (set 1) or from 30ºC to 160ºC (set 2) at a rate of 10ºC/min rate, The specimens were then held at their target temperatures for 30 minutes before cooling back to 30ºC at a rate of 10ºC/min. The molecules at the joining interface in each part are likely to diffuse into the other part under the effect of heat and pressure. Higher the temperature or pressure is, higher is the probability of effective diffusion. In this study, the pressure was kept same in both the press repairs, but temperature was changed. Higher temperature is likely to facilitate more diffusion, leading to a more efficient repair. This was measured via DCB test.

The process is shown schematically in Figure 6.

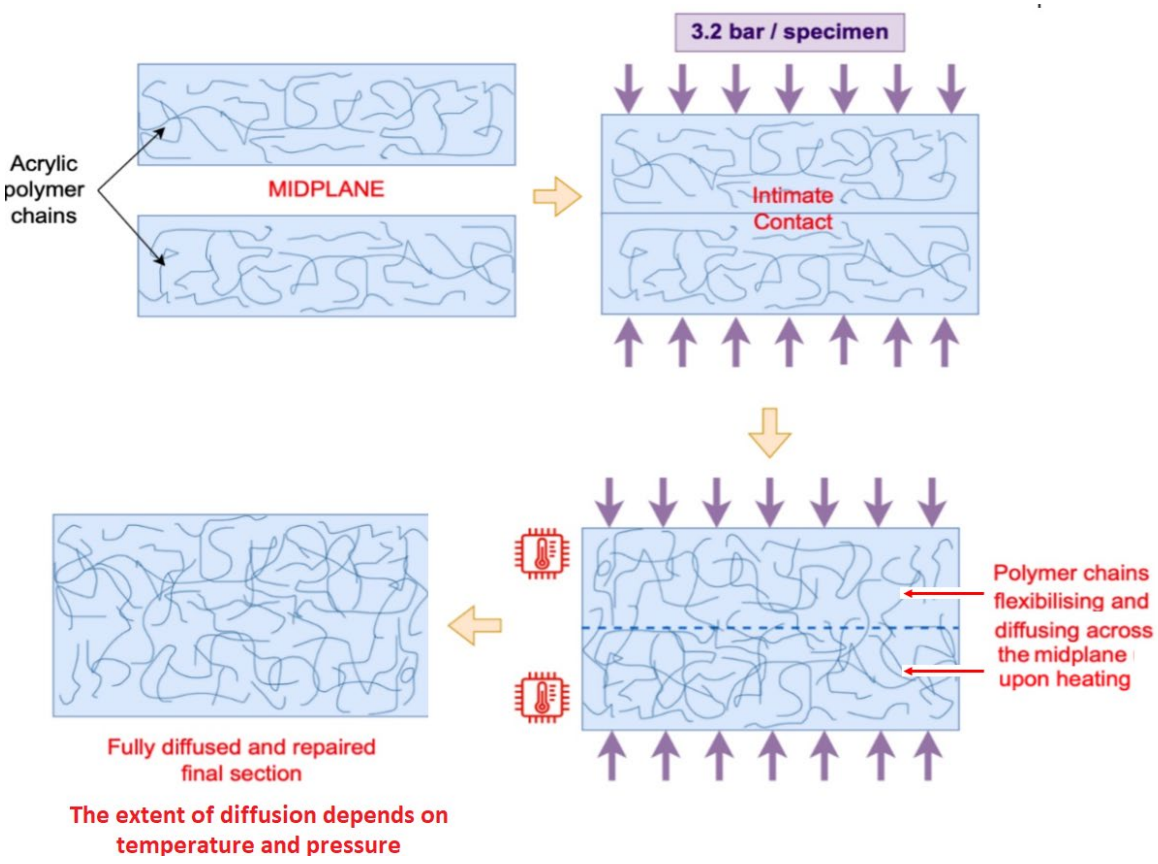

Fig. 6. *Schematic diagram of the fusion bonding mechanism during heated press repair*

The specimens' post-repair widths and thicknesses remained within 2 decimal points of original measurements; hence, dimensional changes were neglected. The pre-crack film remained in place and the pre-crack area remained open after the press.

3. Results and Discussion

The mode-I fracture toughness of the virgin GF/acrylic specimens and the repaired specimens were investigated in this work via DCB testing. The name conventions of the specimens used in this work are given below:

- Specimen repaired by resin injection: 'RI Specimen'.
- Specimen repaired at 130ºC under press: '130P Specimen'.
- Specimen repaired at 160ºC under press: '160P Specimen'.

For comparison between the groups, all calculated values below correspond to the 0-35mm crack length (a) range, from pre-crack tip ($a_0 = 0$). This is because 35mm was the maximum tested delamination length of RI specimens. The Load-Displacement curves are direct indicators of crack growth behaviour in DCB tests. Recorded tip opening displacements (δ) were plotted against corresponding applied loads (P) to maintain the constant 5 mm/min extension rate, at each 0.1s instance. The representative curves for each set of specimens are presented in Figure 7.

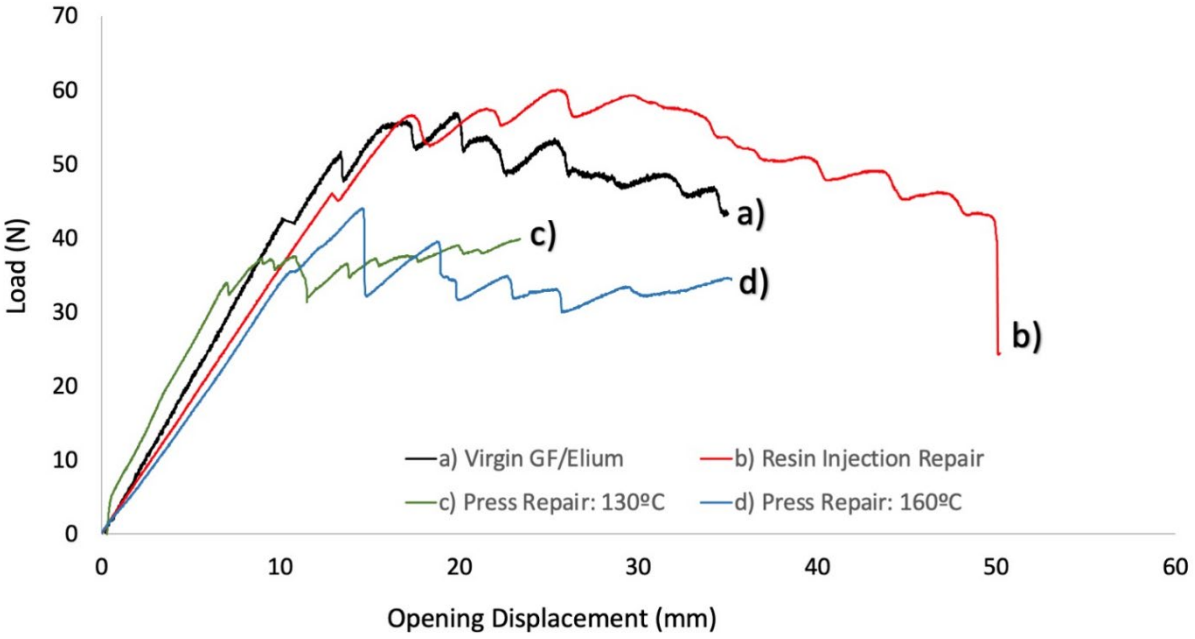

Fig. 7. *Representative Load-Displacement curves of a) virgin b) RI c) 130) d) 160P*

Prior to crack propagation, each set of specimens demonstrated a linearly increasing trend. At this stage, specimen openings and corresponding loads were increased steadily, until the crack-initiating load was reached at the pre-crack tip. Lower peak loads for 130P (39.8 N) and 160P (43.8N) specimens were observed compared to virgin specimens (56.4N), indicating fracture toughness properties could not be fully restored after heated press repairs. Especially for 130P specimens, the results indicate low levels of molecular inter-diffusion and weak bonding at the repair bond line. Meanwhile, RI specimens did not only recover the virgin peak load but exceeded it (60.1N), revealing a toughening effect introduced via resin injection repair. The maximum opening displacements and crack propagation times (up to 35 mm crack length) were mostly proportional to peak loads (Table 2). The delamination time for a fixed crack length is another direct indicator of fracture resistance and the results further prove toughening via resin injection. Under lower loads, 160P specimens showed slightly longer crack times and displacements compared to virgin specimens, revealing that bonding was achieved to a certain extent.

Table 2. *Tip displacement (δ) and total delamination time at 35mm crack mark (a = 35mm), for 4 sets of specimens*

	Virgin	RI	130P	160P
Maximum Displacement	34.9 mm	50.1 mm	23.4 mm	35.2 mm
Propagation Time	413 s	598 s	281 s	422 s

Upon crack initiation, all four curves (Figure 7) exhibited a *jagged* pattern, which is indicative of unstable crack propagation [10]. These trends show similarity to most thermoplastic composites DCB results in published literature [11]. It is evident that the crack growth advances discontinuously in a series of rapid growth and arrest phases, in terms of load drops and small oscillations, which reveals *stick-slip behaviour* [12]. A stick-slip mechanism in composite fracture is caused by the delaminated surfaces' sporadic sliding and locking during crack propagation due to factors such as surface roughness and presence of interfacial bonding and/or fibre-bridging [13]. The crack tip proceeds haltingly because of this irregular "sticking" and "slipping", causing fluctuations in load and displacement measurements. Moreover, these rapid oscillations may also be due to interlaminar discontinuities, such as GF fabric twists, gaps, or crimps, which can develop localised tough or vulnerable spots along the crack path [14].

The highest extent of fibre bridging was observed in virgin specimens (Figure 8a). Fibre bridging is a fracture mechanism in which the fibres that stretch between the delaminating surfaces resist crack propagation by transferring stresses across the mid plane. Existing fibres are broken as the crack advances, but some of these continue to tie both sides to some extent and act as a "bridge" in tension against the crack gap extension [15]. RI specimens showed similar behaviour to their virgin counterparts, indicating that the interlaminar structure behaved similarly after resin injection repair. In both curves, upon attaining peak load, an overall load reduction was observed with increasing opening displacement. This is attributed to elastic energy stored by the composite being released after the onset of crack propagation [16]. However, less fibre-bridging was visible in RI specimens, as most fibre

bridges were ruptured during virgin testing (Figure 8b). Hence, stick-slip behaviour of RI specimens was most likely due to ductile deformation of the injected in-situ thermoplastic layer, as well as varying concentrations of semi-interpenetrating network formation along the crack plane. The sharp drop at the end of the curve (Figure 7) represents the *snapping of* RI specimens at the 35mm delamination mark.

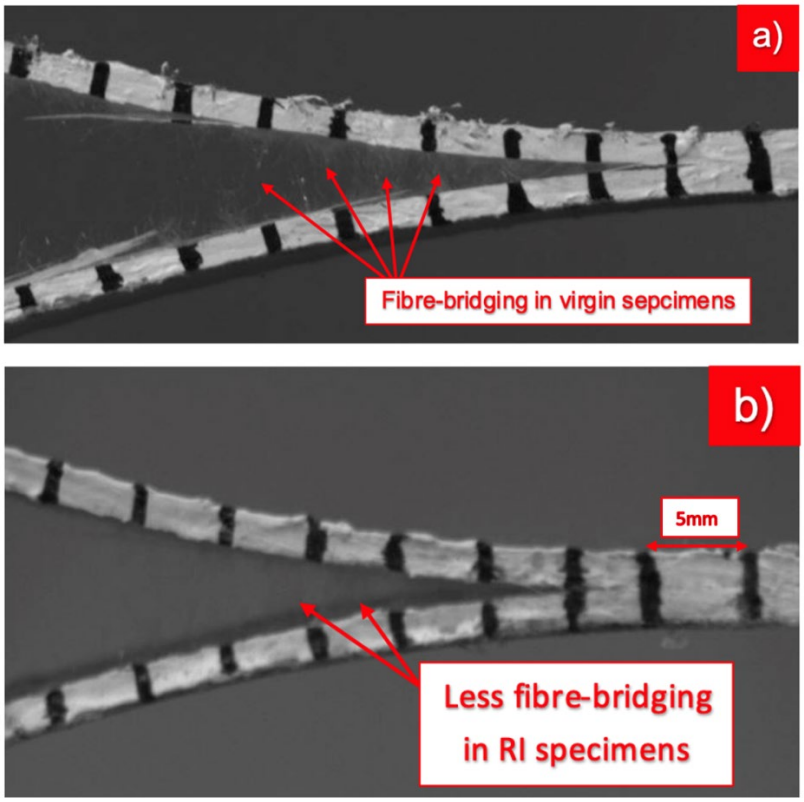

Fig. 8. *Fibre-bridging observed in a) virgin specimens; b) in RI specimens*

The 160P specimens displayed sharper load drops against extension (Figure 7), revealing fast crack jumps, which may indicate that fusion bonding of specimens did not occur uniformly across the mid plane. The 130P specimens exhibited a flatter curve (Figure 7) than other specimens during crack propagation. This might be due to the fact that pressure was not distributed uniformly during repair, with increased contact deeper into the crack zone, i.e., further away from press plate edges (please refer to Figure 5). These effects are less pronounced for 160P specimens, as higher inter-diffusion levels and stronger interlaminar bonding were achieved at the higher temperature. Higher fibre-bridging effects were seen in

160P specimens compared to 130P, which further explains higher test loads for the former (Figure 9).

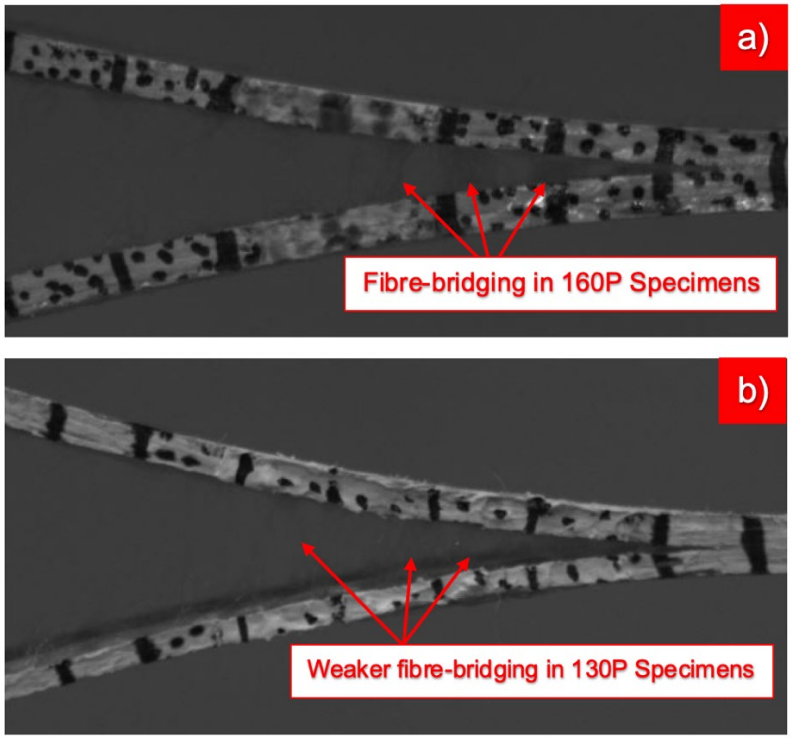

Fig. 9. *Fibre-bridging observed in a) 160P specimens; b) 130P specimens*

The interlaminar mode-I fracture toughness of a composite can be expressed in terms of strain energy release rate (G_{IC}), i.e., the critical energy value required to maintain crack propagation at any distance from loading point. Modified Beam Theory (MBT) is the most often reported method in literature for calculating mode-I fracture toughness of composites. DCB results were calculated using both MBT and NL methods. RI specimens exhibited the highest mean $G_{IC\text{-}Init}$ (for initiation) and $G_{IC\text{-}Prop}$ values (for propagation), with 537.05 J/m^2 and 1465.77 J/m^2 respectively. The results concluded a 23% increase in $G_{IC\text{-}Init}$ and 33% increase in $G_{IC\text{-}Prop}$ of RI specimens compared to virgin specimens that showed a $G_{IC\text{-}Init}$ of 413.38 J/m^2 and $G_{IC\text{-}Prop}$ of 977.84 J/m^2. This is an important finding that indicates GF/acrylic composites that are repaired with resin injection are able to resist higher energy rates compared to virgin coupons, even if some fibres are broken or damaged in that region. Resin injection repair cannot reverse the effect of fibre breakage or damage in a composite but can heal the cracks most efficiently

leading to a high repair efficiency. These results verify previously theorised toughening effects of thermoplastic semi-IPNs, offering the potential for effective on-site repair of acrylic based large thermoplastic composite structures.

As for 160P specimens, $G_{IC\text{-}Init}$ and $G_{IC\text{-}Prop}$ values were 309.59 J/m^2 and 607.46 J/m^2 respectively, exhibiting 74% and 62% mode-I fracture toughness recovery compared to the virgin state. These results align well with reference studies [8]. The values were lowest for 130P specimens with 56.33 J/m^2 of $G_{IC\text{-}Init}$ and 284.64 J/m^2 of $G_{IC\text{-}Prop}$, proving that 130ºC is an insufficient temperature to induce fusion bonding repair of debonded interlaminar surfaces of acrylic/GF composites at 3 bar pressure and 60 min time. The representative resistance curves (R-curves) and charts comparing mean mode-I fracture toughness values are presented in Figures 10 and 11 respectively.

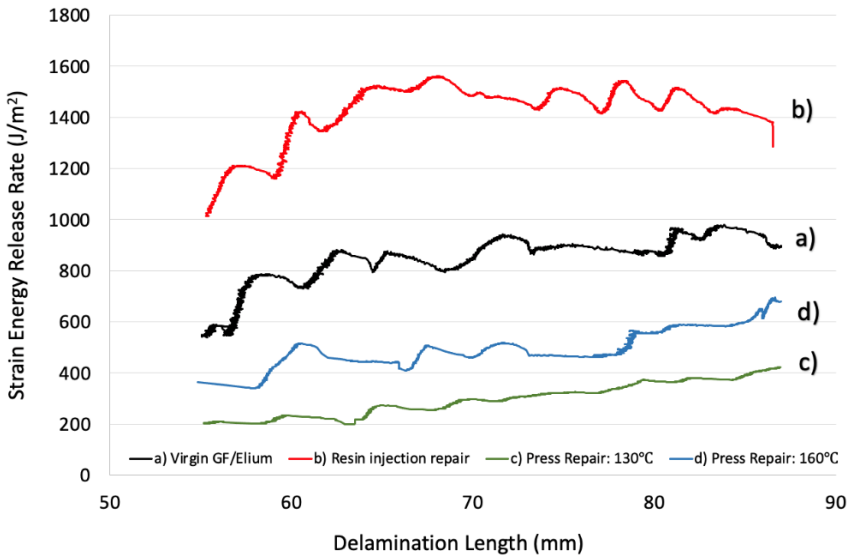

Fig. 10 *Resistance curves obtained from DCB testing of a) virgin acrylic/GF laminates and repaired acrylic/GF laminates (b)resin injection repaired or RI, (c) press repaired at 160 C or 160P and (d) press repaired at 130C or 130P).*

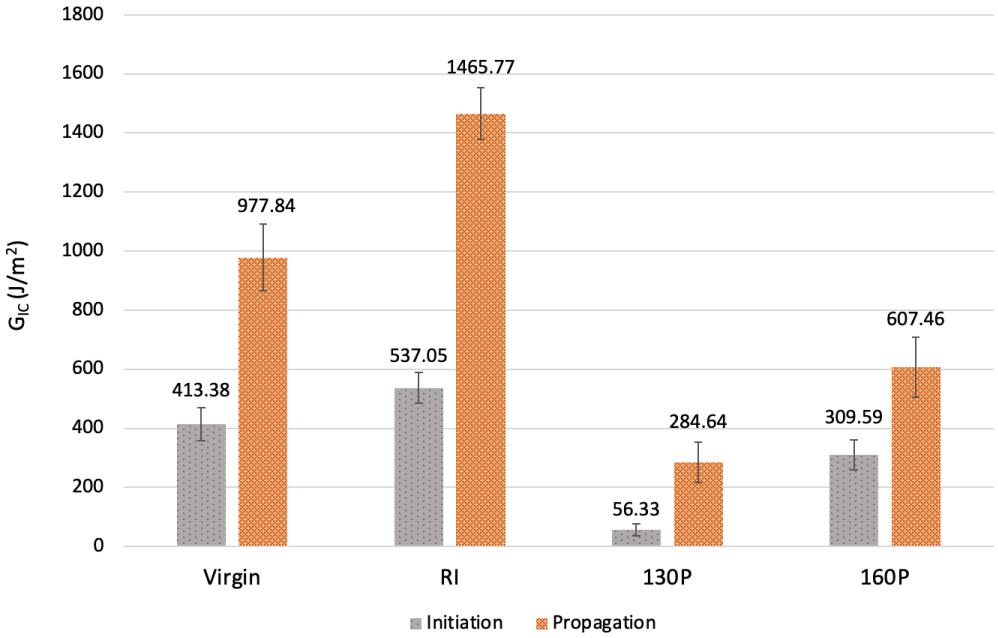

Fig. 11. *Comparison of mean* $G_{IC\text{-}Init}$ and $G_{IC\text{-}Prop}$ values for 4 DCB test groups.

All R-curves in Figure 10 were trimmed to start at the longest pre-crack distance between 4 groups (55 mm) and to end at shortest crack length (87mm) for coherency.

Curves of virgin and RI specimens appeared to remain relatively constant over the plateau region (Figure 10). It is believed that the fracture toughness of damaged virgin specimens was further increased by resin injection because the added acrylic layer transferred the crack locus throughout its thickness before reaching the original separated surfaces [17]. Long polymer chains forming the semi-IPNs enhanced the ductility of the mid plane area, developing a tough 'buffer' layer that sits on the crack path, providing increased material resistance [18]. It is also likely that injected resin formed strong bonds with some ruptured acrylic-compatible fibres, further improving interlaminar stiffness. Sudden drops in RI specimen curve (Figure 11) might have occurred due to entrapped air bubbles in the injected resin mixture.

R-curves of 130P and 160P showed more visible G_{IC} increases, which further supported the hypothesis that higher pressures and stronger bonding were achieved deeper into the crack, towards the press plate centre (Figure 7). According to previous studies on acrylic composites, uneven pressure distributions can result in the formation of resin-rich sites and micro voids, which considerably reduce DCB performance of laminates, as observed here with press-

repaired specimens [8], [18]. Low G_{IC} values for 130P specimens suggest spontaneous and rapid crack growth, i.e., crack jumping, due to minimal bonding of separated surfaces [19]. As seen in Figure 9, greater fibre-bridging was observed in 160P specimens compared to 130P, with increased healing temperature, resulting in higher fracture toughness values. This increase in fibre bridges can be attributed to greater inter-diffusion of polymer chains in 160P sample across the joining layer, due to higher thermal energy, forming a stronger bond line in the region than that in 130P [20]. These fibre-bridges were much shorter and failed under smaller loads than those observed in virgin specimens, as most fibres in second DCB test were already broken.

These results show that it is challenging and energy-intensive to restore fracture toughness via heated pressing, as damaged fibres in the mid plane remain broken and there is not any additional toughening material involved to compensate for this, unlike with resin injection repair. Hence, recovery ratios solely depend on the amount of supplied energy, i.e heat and pressure, and time.

In summary, the mode-I fracture toughness evolution of 4 DCB groups is associated with toughening mechanisms of fibre-bridging, plastic matrix deformation and resin-rich areas, and consequent secondary energy dissipation processes such as tow rupture (fibre bridge breaking), ductile debonding events and micro voids [14]. Fibre-bridging enhances the composite's energy absorption capacity, and hence its fracture resistance, by serving as a "safety net" that restrains the crack from proceeding further until sufficient loads break the fibres [21]. This effect was most apparent in virgin specimens, as all mid plane fibres were intact during first DCB tests, leading to higher G_{IC} values than press repaired specimens. RI specimens produced the highest results, which demonstrated acrylic polymer’s ability to absorb energy by undergoing plastic deformation during extension, through strong semi-IPN bonds formed with the original resin matrix [15]. Crack deflection into adjacent layers from the midplane could have occurred in this case due to the toughened mid plane [22]. Thus, it was evident that monomeric acrylic resin can facilitate efficient repair of composite structures on-

site or off-site with high recovery of the mechanical properties. All DCB results are shown in the supplementary document (Table S2-S5).

Distinct failure modes and toughening mechanisms were visible in the SEM micrographs as shown in Figure 12. Crack initiation points and propagation regions were analysed. Ductile matrix deformation regions and risers observed in each set confirmed ductile interlaminar fracture behaviour [23]. These properties were most pronounced in RI specimens (Figure 12b), which further demonstrated increased toughening effects of the newly formed semi-IPN networks in the mid plane, after resin injection repair. Consequently, RI specimens displayed the roughest fracture surface topologies (Figure 12b), indicating the highest resistance against crack propagation [24]. This was due to high strain energy absorption capacity of the infused acrylic resin layer, which overlaid the 0º mid plane fibres. Virgin specimens also exhibited rough surfaces, ductile deformation regions and strong fibre-matrix bonding. However, these were less prominent compared to RI specimens (Figure 12a). 130P specimens showed the smoothest fracture surfaces (Figure 12c), where highly irregular resin distributions and poor fibre-matrix *re-bonds* were observed, due to inadequate re-bonding at 130ºC. Evidence of positive toughening effects of increased repair temperature were present in 160P micrographs (Figure 12d), in terms of uniform resin spread and stronger fibre-matrix re-bonding [25]. Several other aspects such as fibre fractures, micro voids and fibre imprints of pulled out fibres were also observed. Lastly, it is important to note that outbursts of 90º fibres through the mid plane were present in all groups. This was most likely due to localised and spontaneous transverse crack jumps into the neighbouring 90º layers during propagation, which also contributed to mild stick-slip behaviour [26].

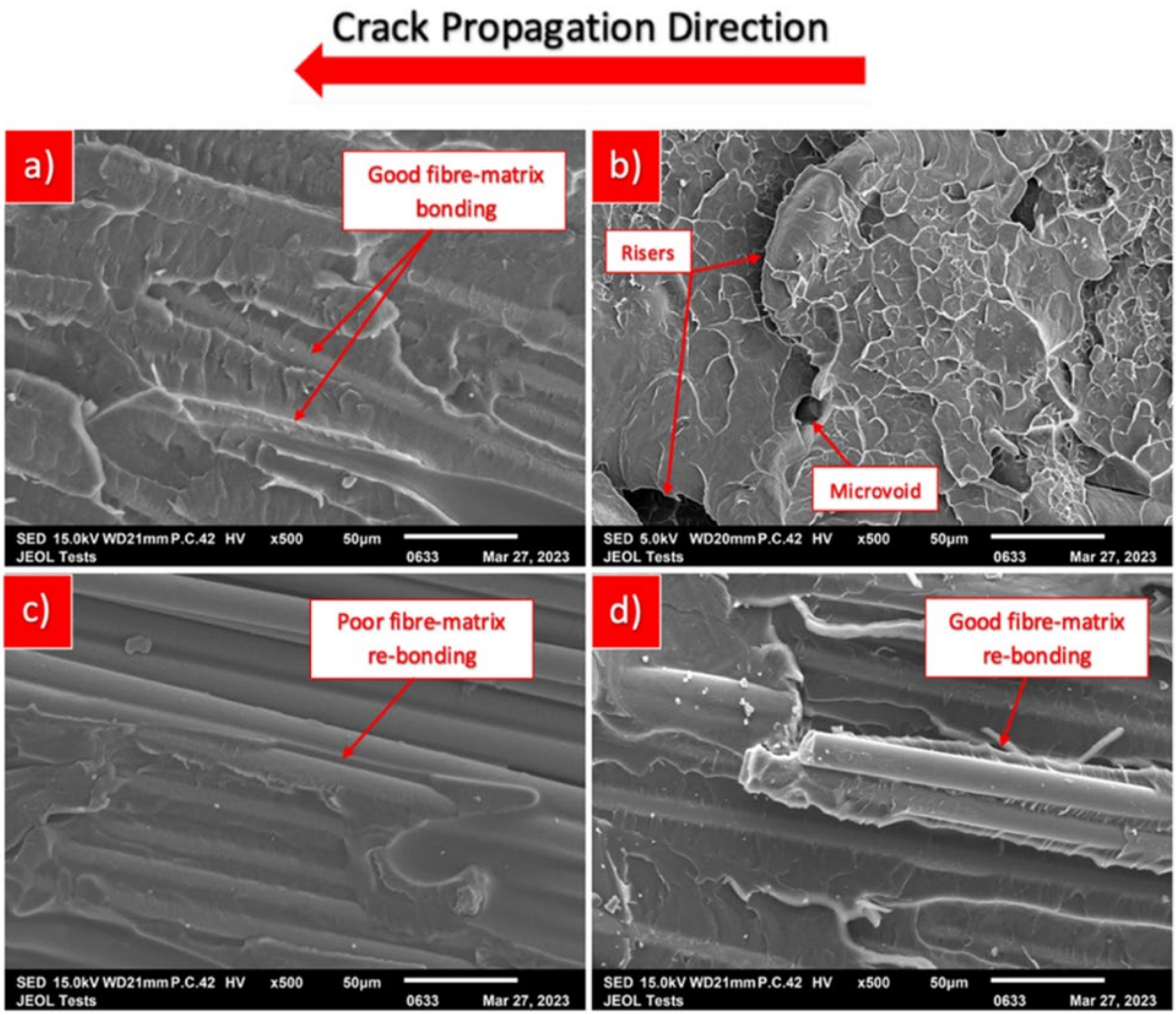

Fig. 12. *Propagation surface micrographs of a) virgin; b) RI; c) 130P; d) 160P specimens at x500 magnification*

4. Conclusion

This study investigated potential repair methods of *in-situ* polymerised acrylic/glass composites. Their crack healing performance was assessed in terms of mode-I fracture toughness recovery via double cantilever beam testing. Two repair methods, liquid resin injection and press moulding, were performed, where the latter was experimented at two different temperatures (130ºC and 160ºC).

The specimens repaired by resin injection exhibited the highest values of $G_{IC\text{-}Init}$ and $G_{IC\text{-}Prop}$, 537 J/m^2 and 1466 J/m^2 respectively. The results showed a 23% increase in $G_{IC\text{-}Init}$ and 33% increase in $G_{IC\text{-}Prop}$, from the virgin state (413 J/m^2 and 978 J/m^2 respectively). This

improvement is associated with semi-interpenetrating network formation and the consequent increase in interlaminar ductility at the repaired bond line. The specimens repaired by press at 160ºC demonstrated 62% fracture toughness restoration from the virgin state, indicating interlaminar integrity could be restored to a certain extent by inter-diffusion of the acrylic polymer chains. The results agreed well with literature and have the potential for improvement under more optimised heat and pressure conditions. The specimens pressed at 130ºC displayed insufficient repair performance, with only 29% fracture toughness recovery. The micrographs captured by scanning electron microscope revealed distinctive fracture behaviours for each set of repaired samples, which provided tangible agreement and support to DCB test results.

Therefore, the presented observations will aid the development of on-site repair methods and recycling strategies, for the reuse of polymer composite structures in the renewable energy sector, and beyond.

References

[1] P. K. Dubey, S. K. Mahanth and A. Dixit, “RECYCLAMINE® - NOVEL AMINE BUILDING BLOCKS FOR A SUSTAINABLE WORLD,” Aditya Birla Chemicals (Thailand) Limited, Rayong, Thailand.

[2] L. Mishnaevsky Jr., “Repair of wind turbine blades: Review of methods and related computational mechanics problems,” *Renewable Energy: An International Journal,* vol. 140, pp. 828-839, 2019.

[3] A. Lebel, A. Saouab, J. Bréard and W. I. Lee, “Modeling and simulation of voids and saturation in liquid composite molding processes,” *Composites Part A: Applied Science and Manufacturing,* vol. 42, no. 6, pp. 658-668, 2011.

[4] M. Hautier, D. Lévêque, C. Huchette and P. Olivier, “Investigation of composite repair method by liquid resin infiltration,” *Plastics, Rubber and Composites,* vol. 39, no. 3-5, pp. 200-207, 2013.

[5] L. Karthikeyan, D. Mathew and T. M. Robert, “Poly(ether ether ketone)-bischromenes: Synthesis, characterization, and influence on thermal, mechanical, and thermo mechanical properties of epoxy resin,” *Polymers for Advanced Technologies,* vol. 30, no. 4, pp. 1061-1071, 2019.

[6] G. Xian and Z. Wang, “2.17 Carbon Fiber Reinforced Plastics – Properties,” *Materials Science and Materials Engineering,* vol. 2, no. 2, pp. 342-359, 2018.

[7] A. Siddique, Z. Iqbal, Y. Nawab and K. Shaker, “A review of joining techniques for thermoplastic composite materials,” *Journal of Thermoplastic Composite Materials,* vol. 1, no. 38, 2022.

[8] T. Khan, M. Irfan, W. Cantwell and R. Umer, “Crack healing in infusible thermoplastic composite laminates,” *Composites Part A,* vol. 156, 2022.

[9] D. Roy, C. O. Bradaigh, K. O'Rourke and W. Obande, “Method for Joining Thermoplastic Articles”. Scotland, UK Patent WO 2023/017267 A1, 16 February 2023.

[10] J. Chen, E. Schulz, J. Bohse and G. Hinrichsen, “Effect of fibre content on the interlaminar fracture toughness of unidirectional glass-fibre/polyamide composite,” *Composites Part A: Applied Science and Manufacturing,* vol. 30, no. 6, pp. 747-755, 1999.

[11] W. Obande, D. Mamalis, D. Roy, L. Yang and C. M. O Bradaigh, “Mechanical and thermomechanical characterisation of vacuum-infused thermoplastic- and thermoset-based composites,” *Materials & Design,* vol. 223, no. 223, 2019.

[12] D. Tzetsis, P. Hogg and M. Jogia, “Double cantilever beam Mode-I testing for vacuum infused repairs of GFRP,” *Journal of Adhesion Science and Technology,* vol. 17, no. 3, pp. 309-328, 2012.

[13] E. E. Gdoutos, C. A. Rodopoulos and J. R. Yates, “Approximate Determination of the Crack Tip Plastic Zone for Mode-I and Mode-II Loading,” in *Problems of Fracture Mechanics and Fatigue: A Solution Guide* , Springer, 2003, pp. 75-79.

[14] F. Bensadoun, I. Verpoest and A. van Vuure, “Interlaminar fracture toughness of flax-epoxy composites,” *Journal of Reinforced Plastics and Composites,* vol. 36, no. 2, pp. 121-136, 2017.

[15] S. K. Bhudolia, G. Gohel, D. Vasudevan, K. F. Leong and P. Gerard, “Delamination behaviour and surface morphology of wholly thermoplastic composites using different ultra-high molecular weight thermoplastic fabrics with pristine and toughened Elium resin under Mode I loading,” *Composites Part A: Applied Science and Manufacturing,* vol. 164, pp. 1072-1073, 2023.

[16] L. Shanmugam, M. Kazemi, Z. Rao, D. Lu, X. Wang, B. Wang, L. Yang and J. Yang, “Enhanced Mode I fracture toughness of UHMWPE fabric/thermoplastic laminates with combined surface treatments of polydopamine and functionalized carbon nanotubes,” *Composites Part B: Engineering,* vol. 178, 2019.

[17] B. Vieille, M. Chabchoub and C. Gautrelet, “Influence of matrix ductility and toughness on strain energy release rate and failure behavior of woven-ply reinforced thermoplastic structures at high temperature,” *Composites Part B: Engineering,* vol. 132, pp. 125-140, 2018.

[18] S. K. Bhudolia, P. Perrotey and S. C. Joshi, “Mode I fracture toughness and fractographic investigation of carbon fibre composites with liquid Methylmethacrylate thermoplastic matrix,” *Composites Part B,* vol. 134, pp. 246-253, 2018.

[19] Y. Gong, L. Zhao, J. Zhang, Y. Wang and N. Hu, “Delamination propagation criterion including the effect of fiber bridging for mixed-mode I/II delamination in CFRP

multidirectional laminates," *Composites Science and Technology,* vol. 151, pp. 302-309, 2017.

[20] A. Aradian, E. Raphaël and P. de Gennes, "A Scaling Theory of the Competition between Interdiffusion and Cross-Linking at Polymer Interfaces," *Macromolecules - American Chemical Society,* vol. 35, pp. 4036-4043, 2002.

[21] M. Arai, Y. Noro, K.-i. Sugimoto and M. Endo, "Mode I and mode II interlaminar fracture toughness of CFRP laminates toughened by carbon nanofiber interlayer," *Composites Science and Technology,* vol. 68, no. 2, pp. 516-525, 2008.

[22] N. Sela and O. Ishai, "Interlaminar fracture toughness and toughening of laminated composite materials: a review," *Composites,* vol. 20, no. 5, pp. 423-435, 1989.

[23] Y. Huang, Y. Qiu and Y. Wei, "Composite interlaminar fracture toughness imparted by electrospun PPO veils and interleaf particles: A mechanistical comparison," *Composite Structures,* vol. 312, 2022.

[24] B. D. Saz-Orozco, D. Ray and W. F. Stanley, "Effect of thermoplastic veils on interlaminar fracture toughness of a glass fiber/vinyl ester composite," *Polymer Composites,* vol. 38, no. 11, pp. 2501-2508, 2017.

[25] E. S. Greenhalgh, "4 - Delamination-dominated failures in polymer composites," in *Failure Analysis and Fractography of Polymer Composites*, Woodhead Publishing, 2009, pp. 164-194.

[26] Z. Xian-Kui and J. A. Joyce, "Review of fracture toughness (G, K, J, CTOD, CTOA) testing and standardization," *Engineering Fracture Mechanics,* vol. 85, pp. 1-46, 2012.